Fig S1. Concentration of selected elements in the samples RP-2, RP-3, RP5 and NA-5 from the Guanajuato Mining District (GMD) in Mexico

Element	RP-2 [μg/g^{-1}]	RP-3 [μg/g^{-1}]	RP-5[μg/g^{-1}]	NA-5[μg/g^{-1}]
Li	103	122	37.8	61.2
Be	8.80	7.60	2.30	2.60
Na	7710	3730	73.5	10500
Mg	2840	2770	9970	6850
Al	28900	20900	12700	33200
K	15800	16900	1030	12200
Ca	11000	9140	7010	66700
V	122	57.0	50.7	126
Cr	32.3	20.1	30.8	50.0
Mn	747	775	1430	897
Fe	28200	17600	29900	32000
Co	10.6	7.05	12.7	14.7
Zn	205	349	178	240
Ni	18.1	12.7	26.0	30.0
Cu	654	924	705	318
As	53.4	44.3	31.0	42.6
Se	9.80	18.4	6.29	12.8
Sr	59.7	40.1	21.4	234
Ag	50.2	75.3	46.9	36.0
Cd	1.38	2.02	0.76	1.00
Ba	315	247	83.8	289.0
Tl	1.38	1.65	0.28	0.74
Pb	122	260	75.7	238
U	0.97	0.61	0.32	1.11
P	588	479	550	1346
S	786	1240	583	1570
Hg	213	520	622	293
Interstitial Gaseous Elementary Mercury [ng/m^3]	7740 at 20 cm			27700 at 40 cm

Fig. S2. X-ray powder diffraction pattern of the samples RP-2, RP3, RP-5, NA-5 the identified phases are listed in the upper right corner

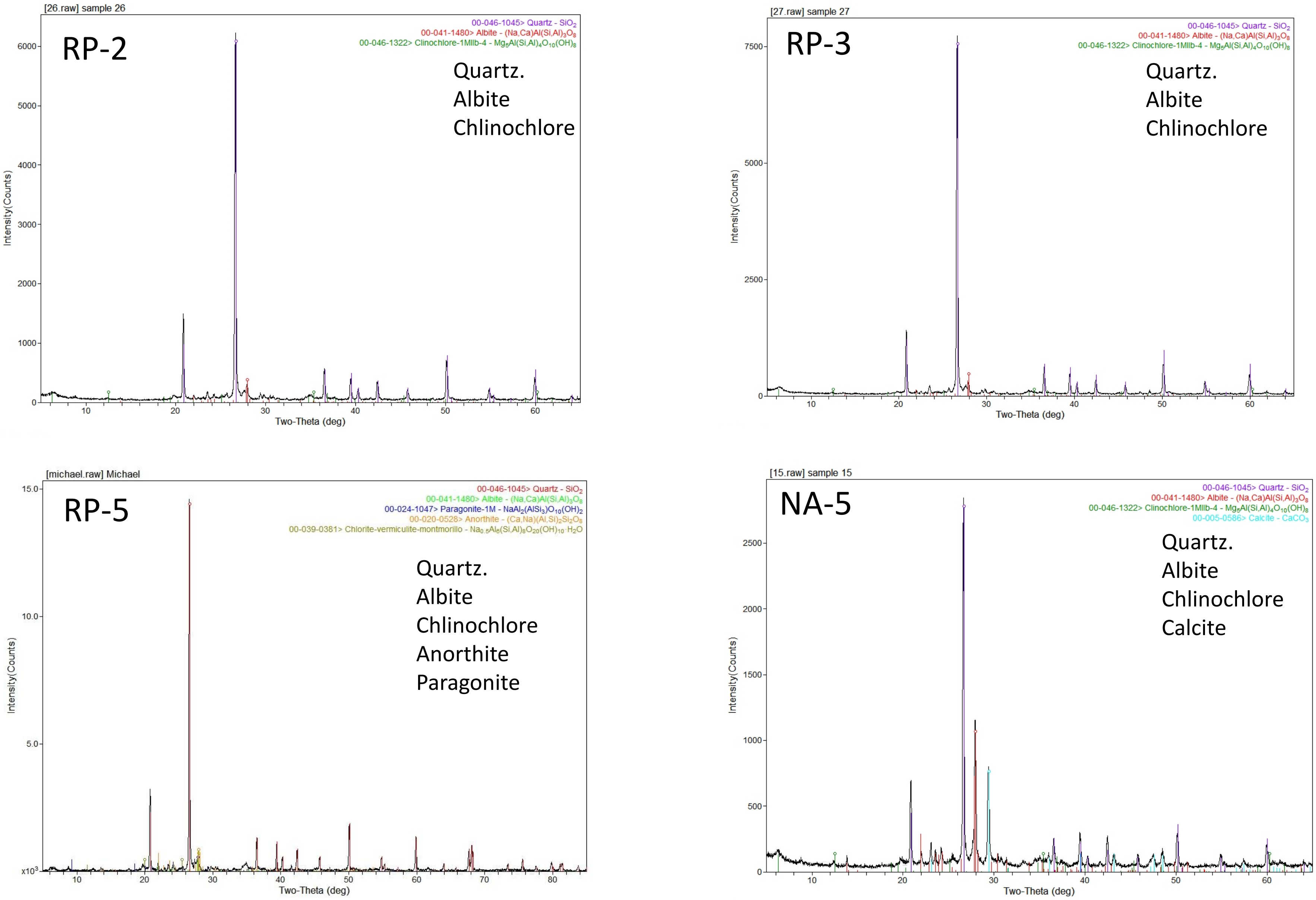

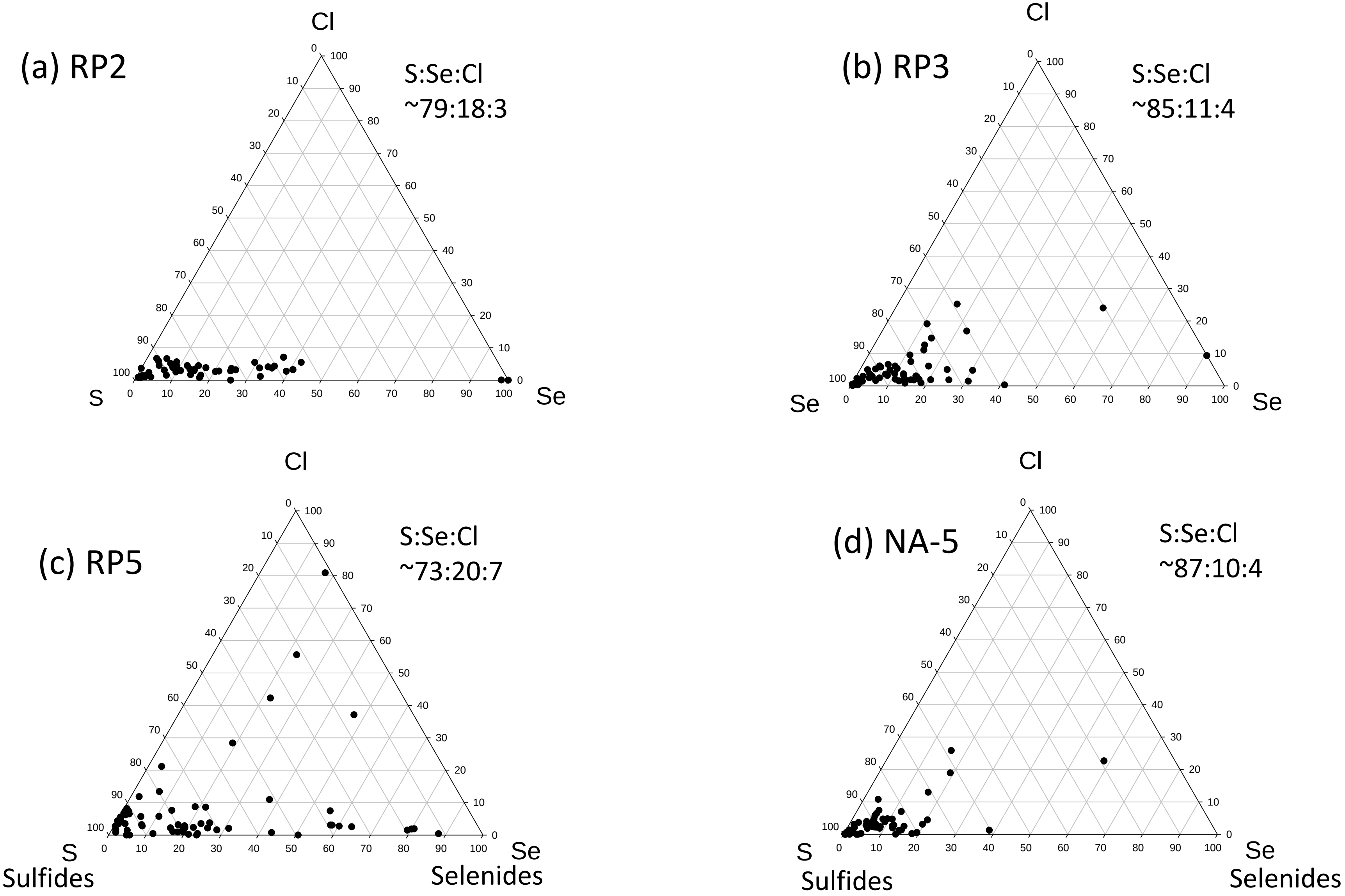

Fig. S3 Ternary diagrams comparing the proportions of S, Se and Cl in Hg-Ag-S-bearing NMA (a) RP-2 (bulk atomic ratio S:Se ~80); (b) RP-3 (bulk atomic ratio S:Se ~ 67), (c) RP-5 (bulk atomic ratio S:Se ~93); and (d) NA-5 (bulk atomic ratio S:Se~123); the average atomic S:Se:Cl ratios for the NMA are indicated.

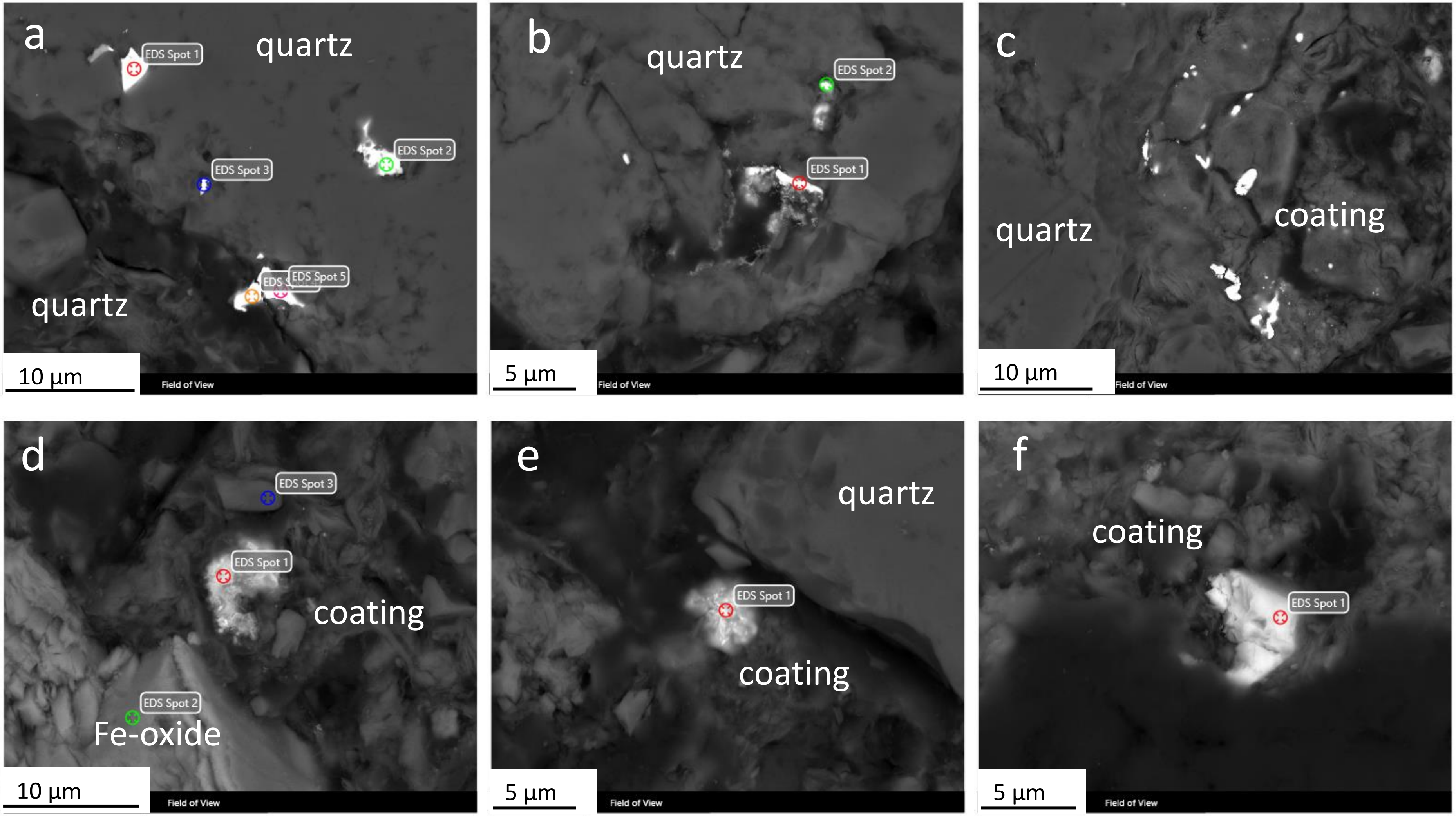

Fig. S4 Examples for the occurrence of Hg nano mineral assemblages: (a)-(b) cracks within quartz grains and (c)-(f) coatings on various mineral grains; locations of underlying grains and coatings are labelled accordingly.

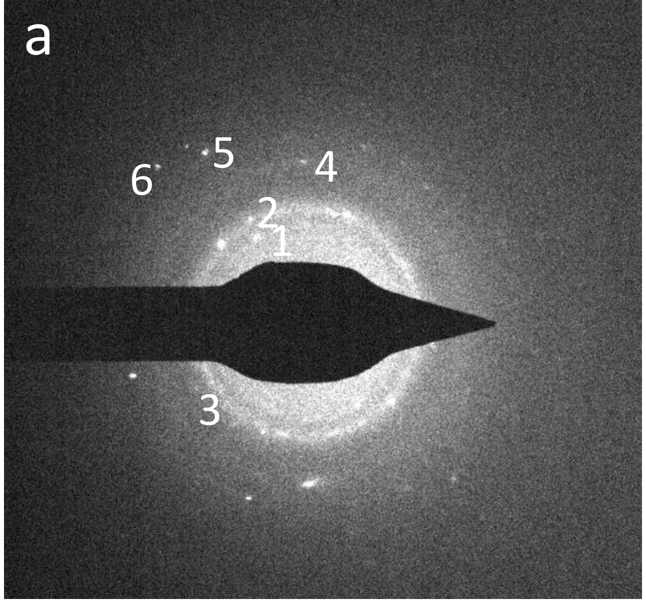

1. d = 2.5 Å
2. d = 2.0 Å
3. d = 1.7 Å
4. d = 1.5 Å
5. d = 1.2 Å
6. d = 1.1 Å

b Matrix composed of 6-line ferrihydrite

n = 5						
at%	Fe	Si	Ca	P	S	Al
lamella 1	69(2)	13(2)	8(1)	7(1)	2(1)	0.8(2)
lamella2	74(4)	14(3)	5(1)	4(1)	3(1)	0.5(2)

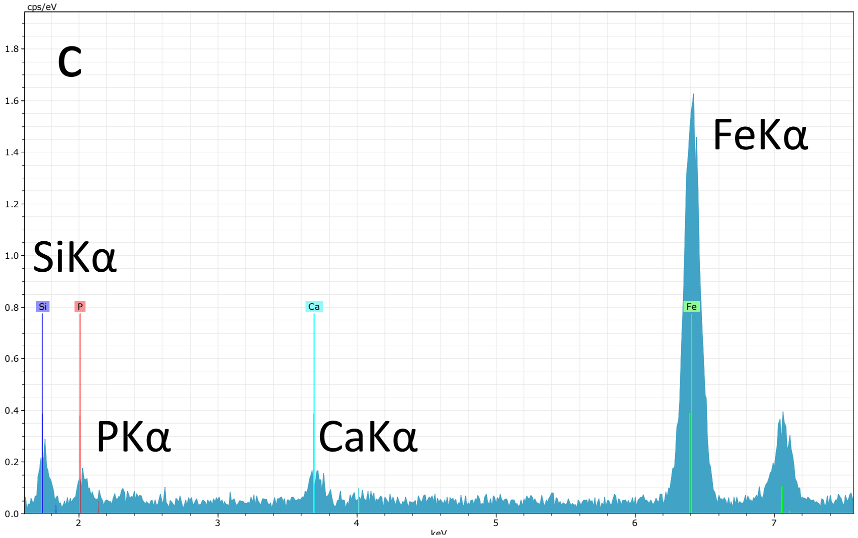

Fig. S5 SAED pattern and chemical composition of the matrix in the FIB lamellae 1 and 2: (a) SAED pattern of the Fe-Si-rich matrix with measured d-spacings, matching those of 6-line ferrihydrite; (b) Average chemical composition (atomic %) of the Fe-Si-rich matrices and (c) an example of a corresponding STEM-EDS spectrum; the lines are labelled accordingly.

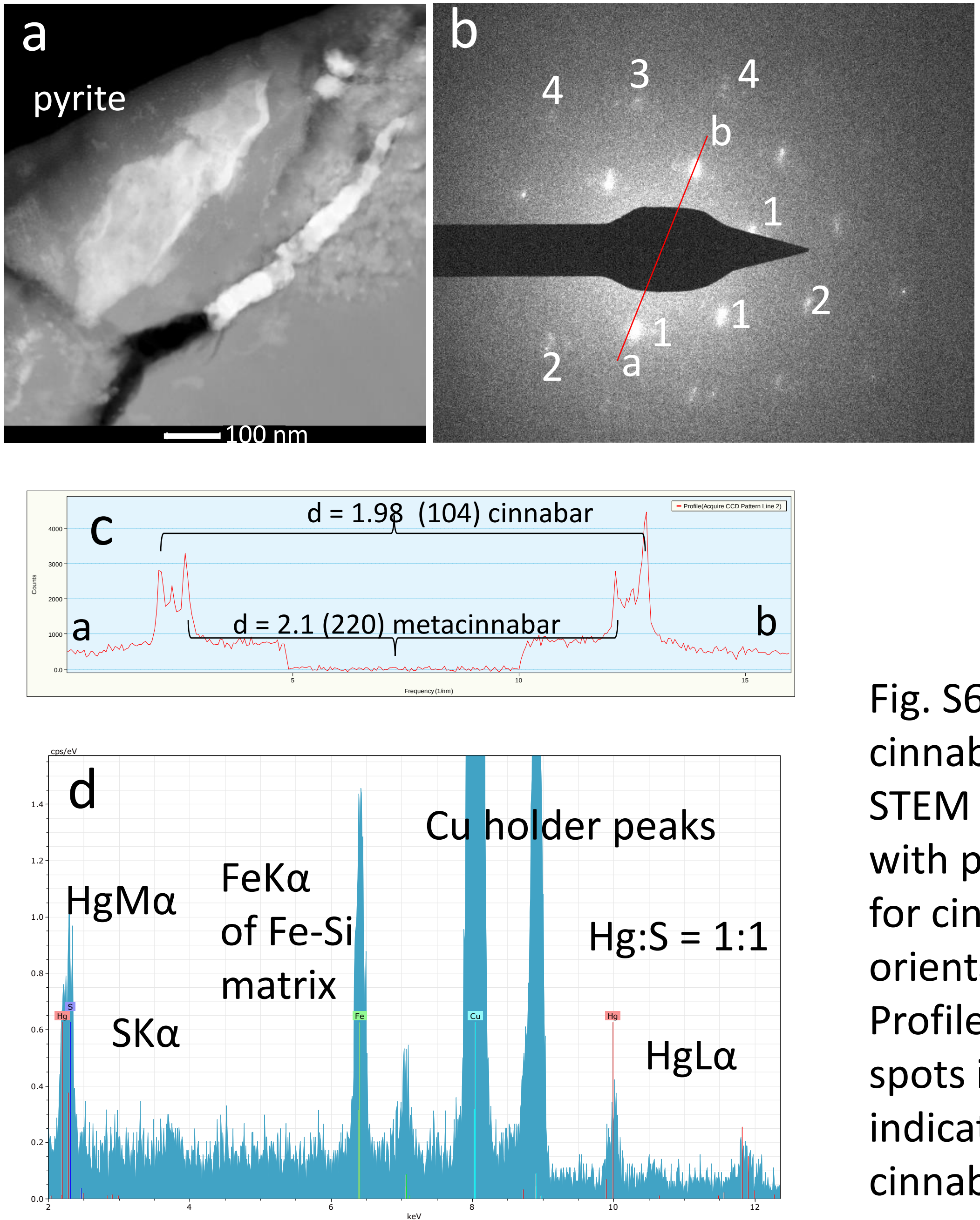

Indexed for cinnabar

1. 1.98/2.1 (104)
2. 1.12 (303)
3. 1.20 (300)
4. 1.00 (208)

Fig. S6 Precipitate of metacinnabar and cinnabar within the Fe-Si-rich matrix: (a) STEM image, (b) corresponding SAED pattern with peaks using the diffraction data reported for cinnabar, a line in the pattern indicates the orientation of the profile shown in (c); (c) Profile across the most prominent diffractions spots in the SAED pattern; the peak splitting indicates d-spacings characteristic for cinnabar and metacinnabar; (d) corresponding EDS spectrum indicating a Hg:S ratio of 1:1.

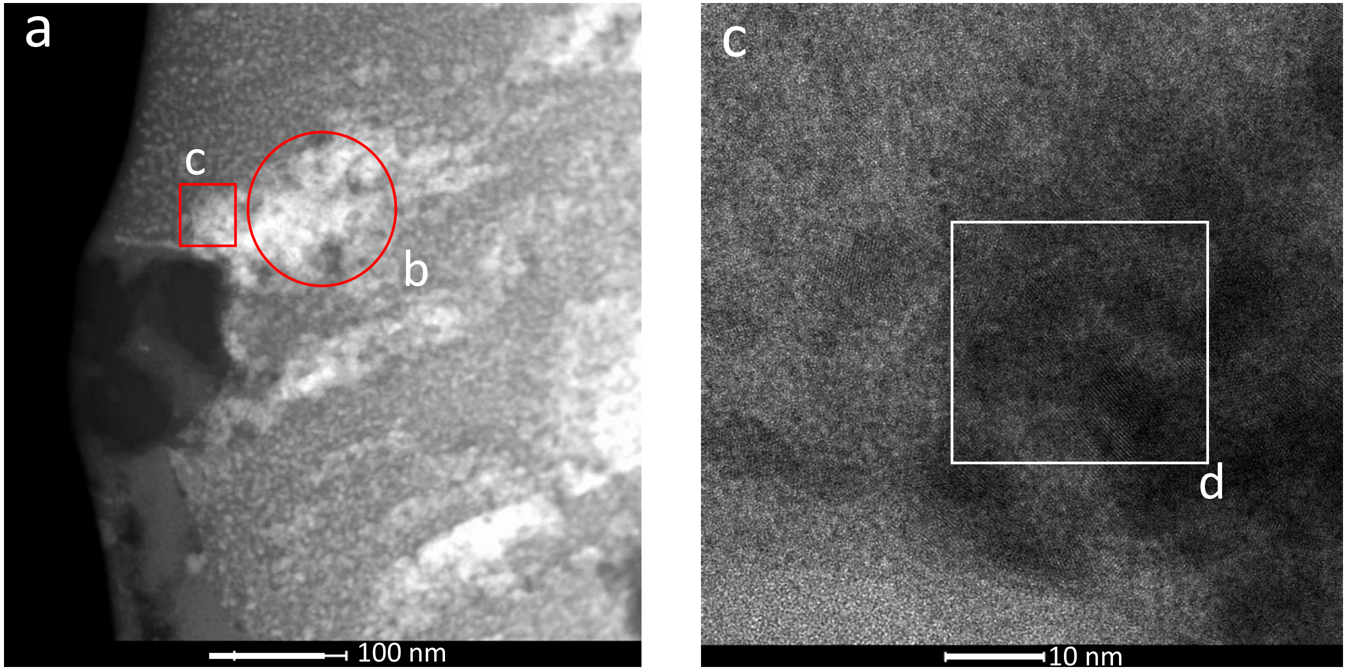

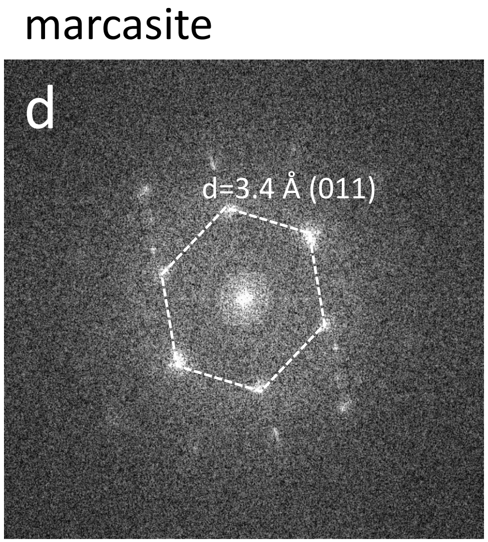

FFT pattern depicting pseudo-hexagonal symmetry of marcasite Structure in the (100) plane

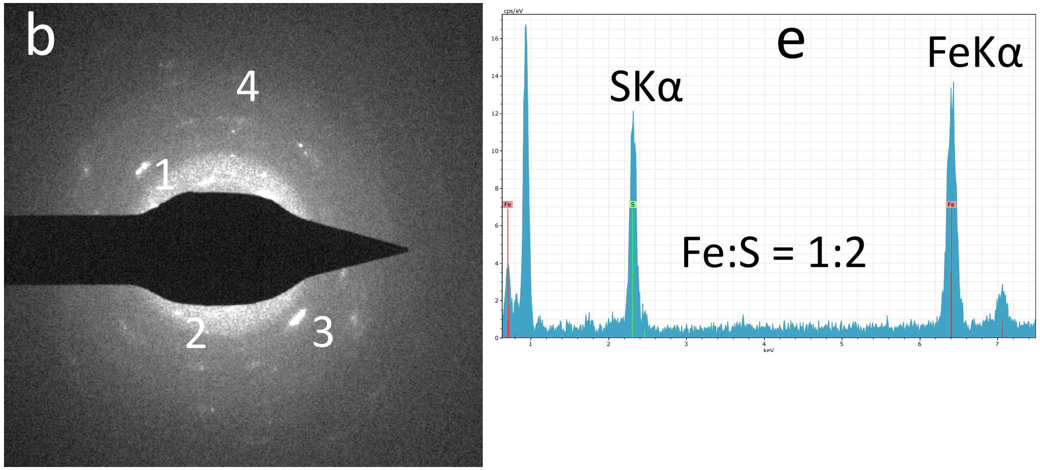

Pyrite
1. d = 3.0 Å (111)
2. d= 2.8 Å (200)
3. d= 2.15 Å (211)
4. d= 1.90 Å (220)

Fig. S7 The occurrence of pyrite and marcasite in lamella 1: (a) STEM image, (b) SAED pattern taken from the encircled area indicated in (a) with d-spacings of the most prominent diffractions spots; (c) HR-TEM image of the area indicated with a white square in (a); (d) FFT pattern of the area labelled in (c), the pseudo-hexagonal symmetry shown by diffraction spots for d=3.4 Å (011) are a characteristic feature of marcasite; (e) an example of a STEM-EDS spectrum of an area composed of pyrite, indicating a Fe:S ratio of 1:2

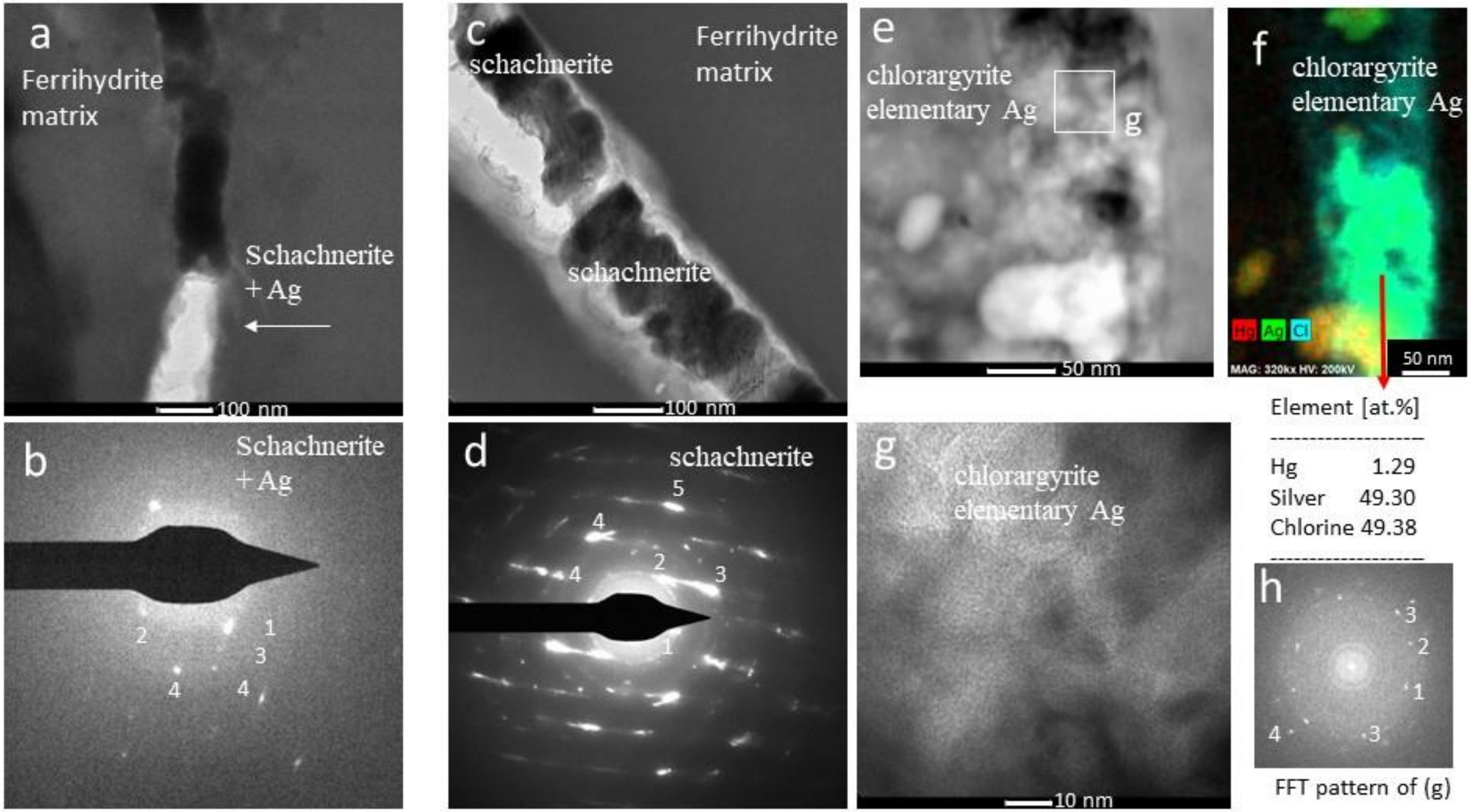

Element	[at.%]
Hg	1.29
Silver	49.30
Chlorine	49.38

FFT pattern of (g)

Measured d-spacings for schachnerite (Schach) and Silver (Ag)

1. d=2.6 Å (321) schach
2. d=2.35 Å (111) Ag
3. d=2.2 Å (101)
4. d=1.5 Å (220) Ag

Measured d-spacings for schachnerite

1. d =2.6 Å(100)
2. d=2.2 Å (101)
3. d=1.35 Å (103)
4. d=1.26 Å (112)

Note: pattern of multiple crystals Ring at d =2.5 Å corresponds to ferrihydrite matrix

Measured d-spacings for chlorargyrite and elementary Ag

1. 3.0 Å (111) chlorargyrite
2. 2.7 Å (200) chlorargyrite
3. 2.35 Å (111) elementary silver
4. 1.93 Å (220) chlorargyrite

Fig. S8 (a), (c) and (g) TEM and (e) STEM images, (f) STEM-EDS chemical distribution maps, (b), (d) SAED and (h) FFT pattern for (a)-(b) schachnerite and native Ag, (c)-(d) schachnerite, (e)-(h) chlorargyrite and elementary Ag; the SAED and FFT pattern in (b), (d) and (h) were taken from (a), (g) and (g), respectively

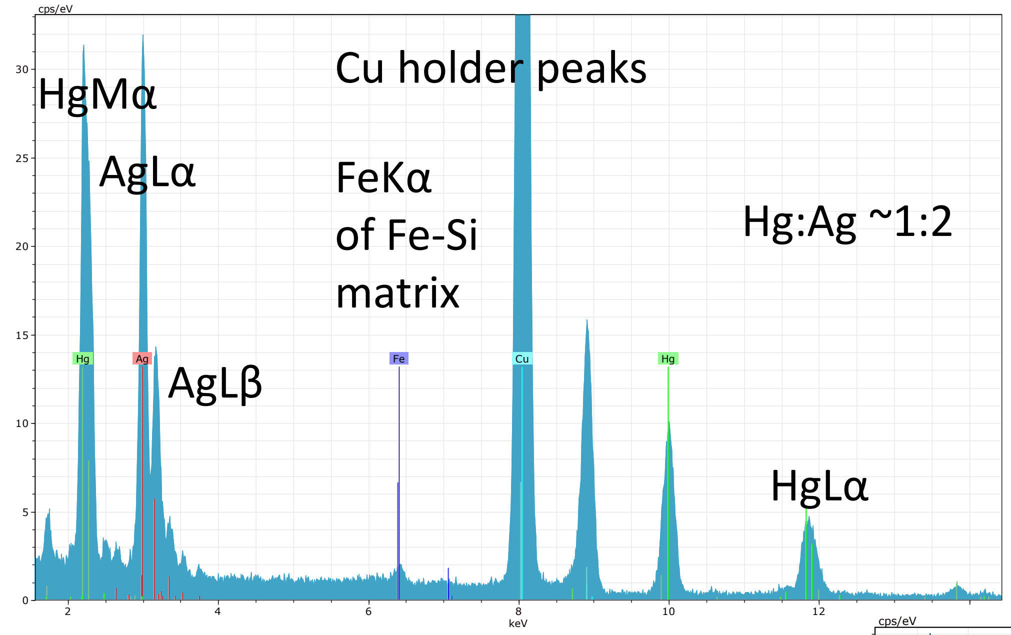

(a) schachnerite
and native Ag

(b) chlorargyrite
with minor HgS
and FeS

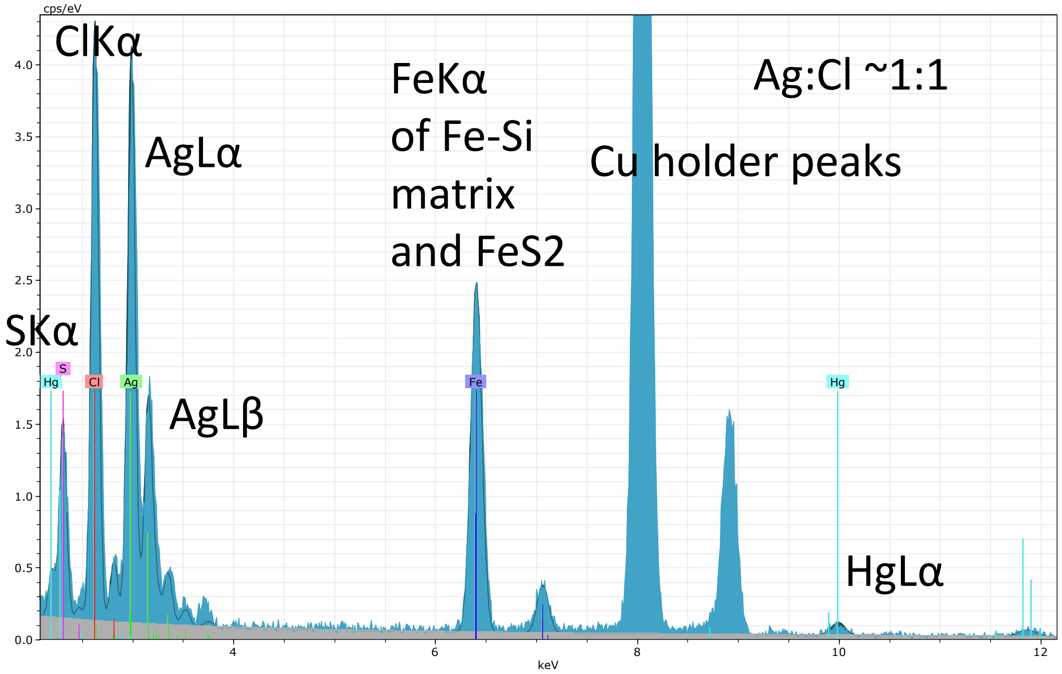

Fig. S9 Examples of STEM-EDS spectra of minerals observed in the confined of lamella 1 (see S8); spectra for (a) schachnerite and native Ag and (b) chlorargyrite with minor HgS and FeS

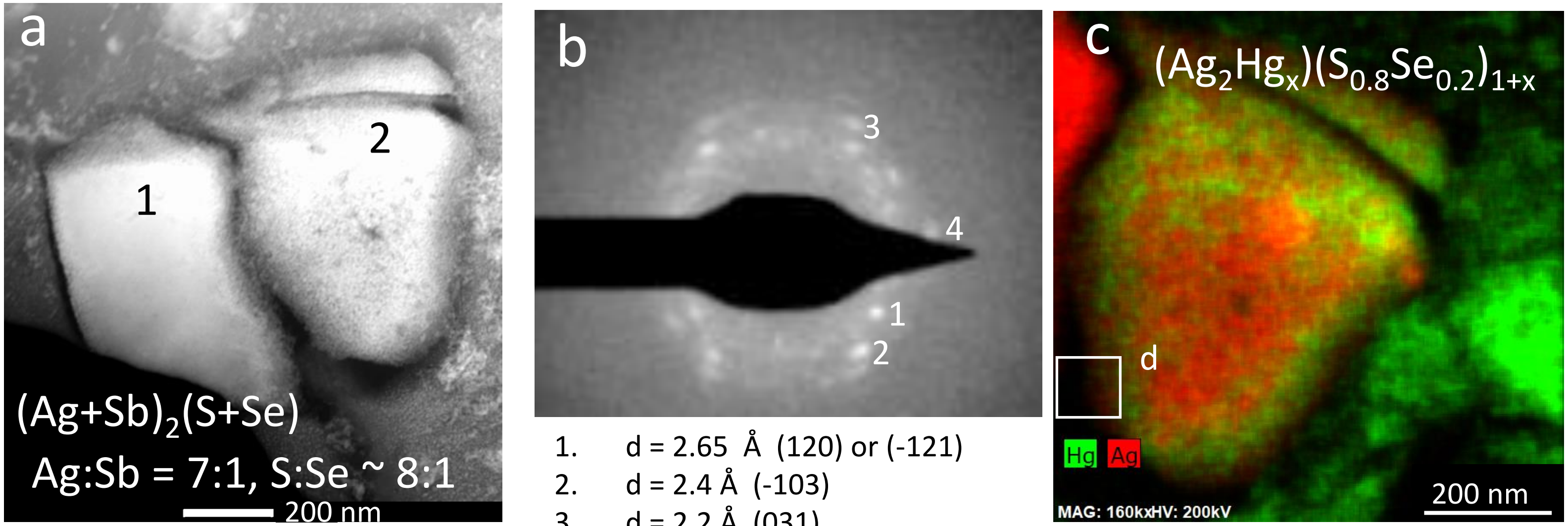

1. d = 2.65 Å (120) or (-121)
2. d = 2.4 Å (-103)
3. d = 2.2 Å (031)
4. d = 2.0 Å (103)

Core

Element	at%
Ag	52.3
Hg	8.0
S	29.8
Se	8.70

Rim

Element	[at.%]
Ag	33.8
Hg	19.5
S	39.2
Se	7.04

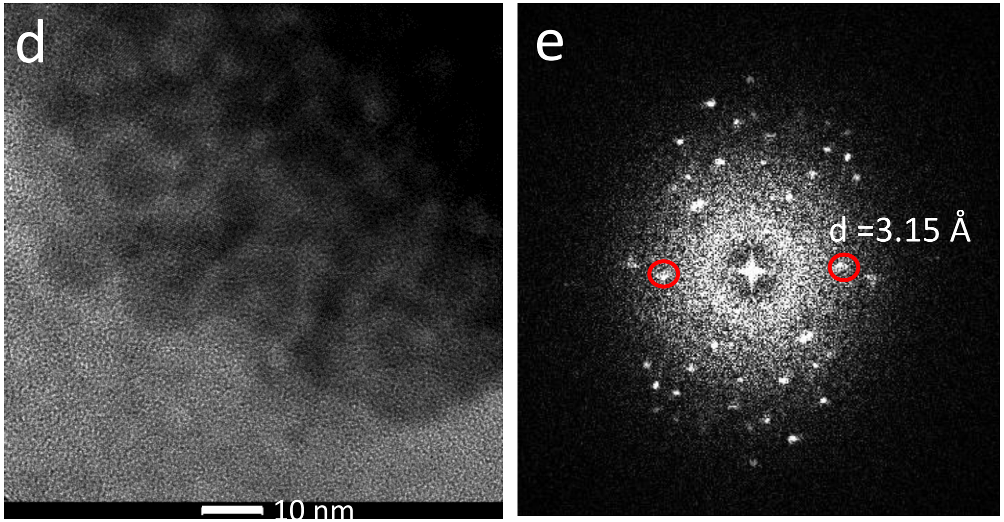

Fig. S10. Altered crystals of acanthite: (a) STEM image and (b) SAED pattern of the less altered acanthite crystal to the left (labelled 1); (c) STEM-EDS chemical distribution maps for Hg (green) and Ag (red) for the crystal to the right (labelled 2), the area shown in (d) is indicated with a white square; (d) HR-TEM image of a Hg-rich area; (e) FFT pattern of (d) indicate the occurrence of NPs of acanthite and a Hg-rich phase, spots at d = 3.15 Å are labelled, the latter d-spacing is not observed for acanthite but occurs for imiterite with d = 3.14 Å (002) or cinnabar with d = 3.17 Å (003).

(a) Interior of crystal 1

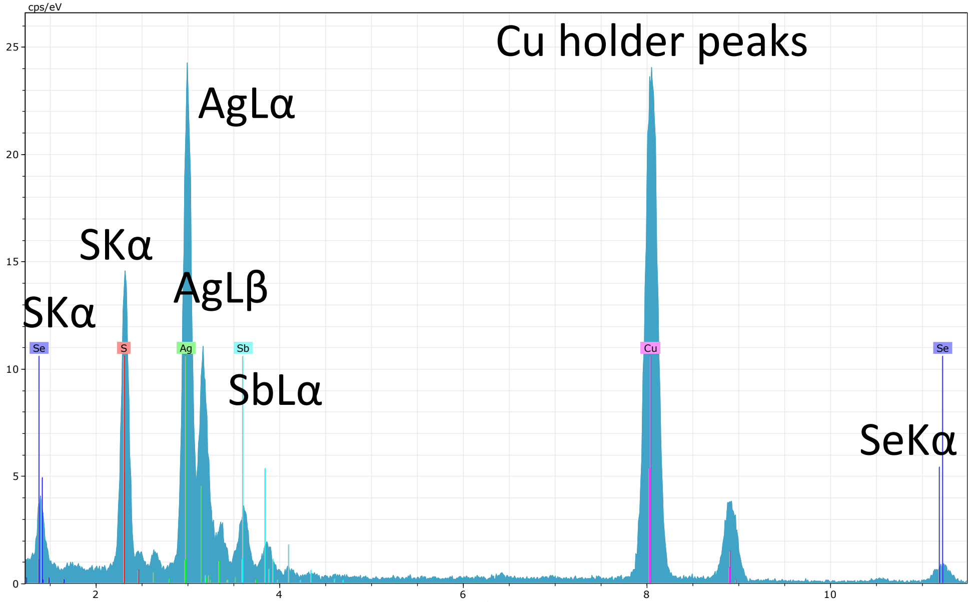

(Ag+Sb):(S+Se) ~ 2:1

S:Se ~ 8:1

(b)Hg-rich rim of crystal 2

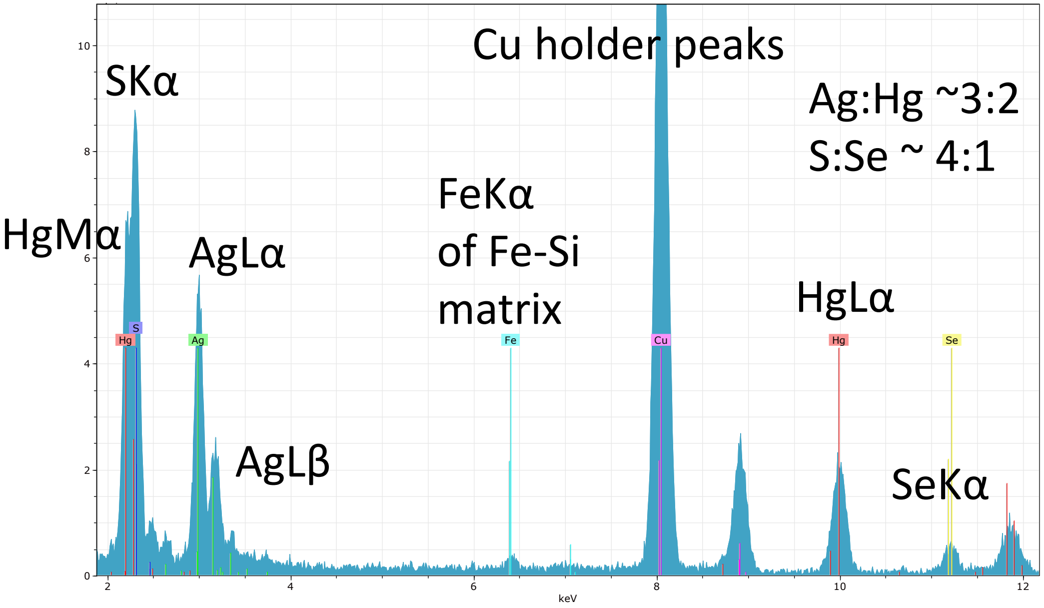

Ag:Hg ~3:2

S:Se ~ 4:1

Fig. S11. Examples of STEM-EDS spectra of selected area within the crystals shown in S10; spectra for (a) the interior of crystal 1 composed of predominantly Ag_2S; (b) altered Hg- and Se-rich rim of crystal 2.

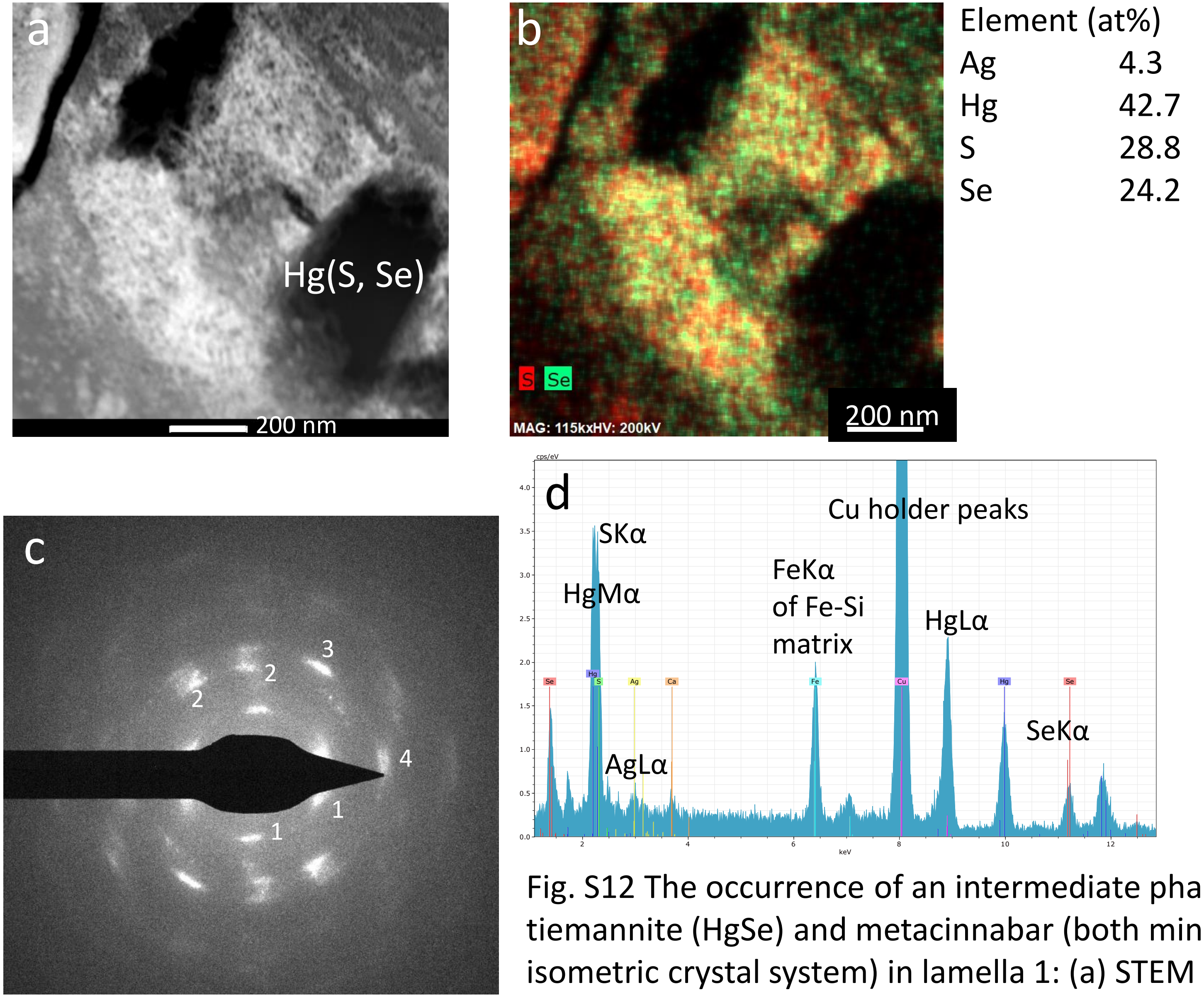

Element (at%)	
Ag	4.3
Hg	42.7
S	28.8
Se	24.2

1. d = 3.55 Å (111)
2. d = 2.2 Å (220)
3. d = 1.85 Å (311)
4. d = 1.78 Å (222)

Fig. S12 The occurrence of an intermediate phase between tiemannite (HgSe) and metacinnabar (both minerals crystallize in the isometric crystal system) in lamella 1: (a) STEM image, (b) STEM-EDS chemical distribution map for S (red) and Se (green) with average elemental composition of the precipitate (semi-quantitative) and (c) SAED pattern with the d-spacings of the most prominent diffraction spots; (d) STEM-EDS spectrum

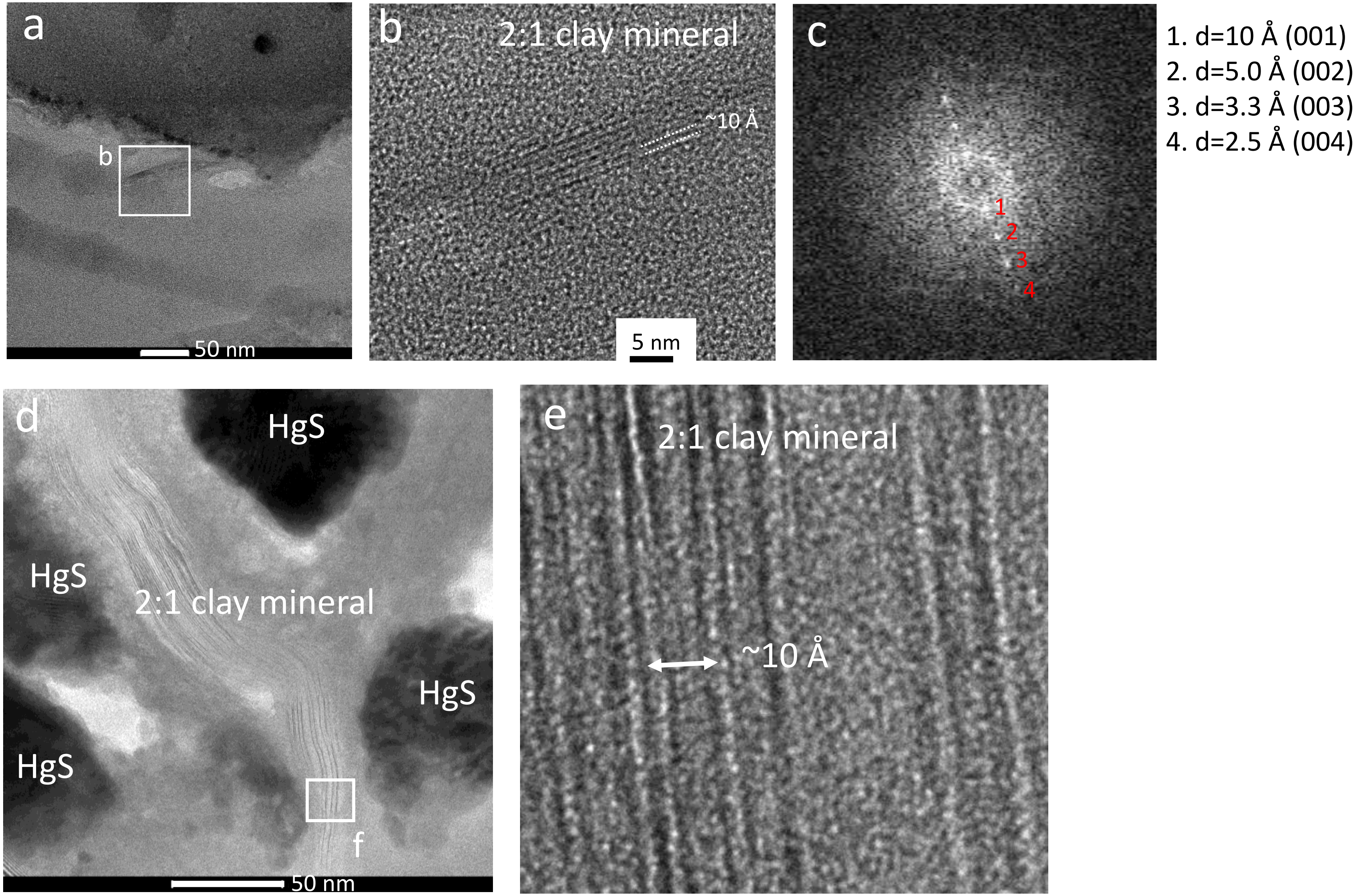

Fig. S13 Clay minerals with 2:1 structure type in (a)-(c) lamella 1 and (d)-(e) lamella 2: (a) TEM image, (b) HR-TEM image of the area indicated in (a); (c) FFT pattern of (b) with d-spacings; (d) TEM image and (e) HR-TEM image of the area indicated in (d); the characteristic d-spacing of d =10 Å for lattice fringes of 2:1 layer silicates is indicated in (b) and (e).

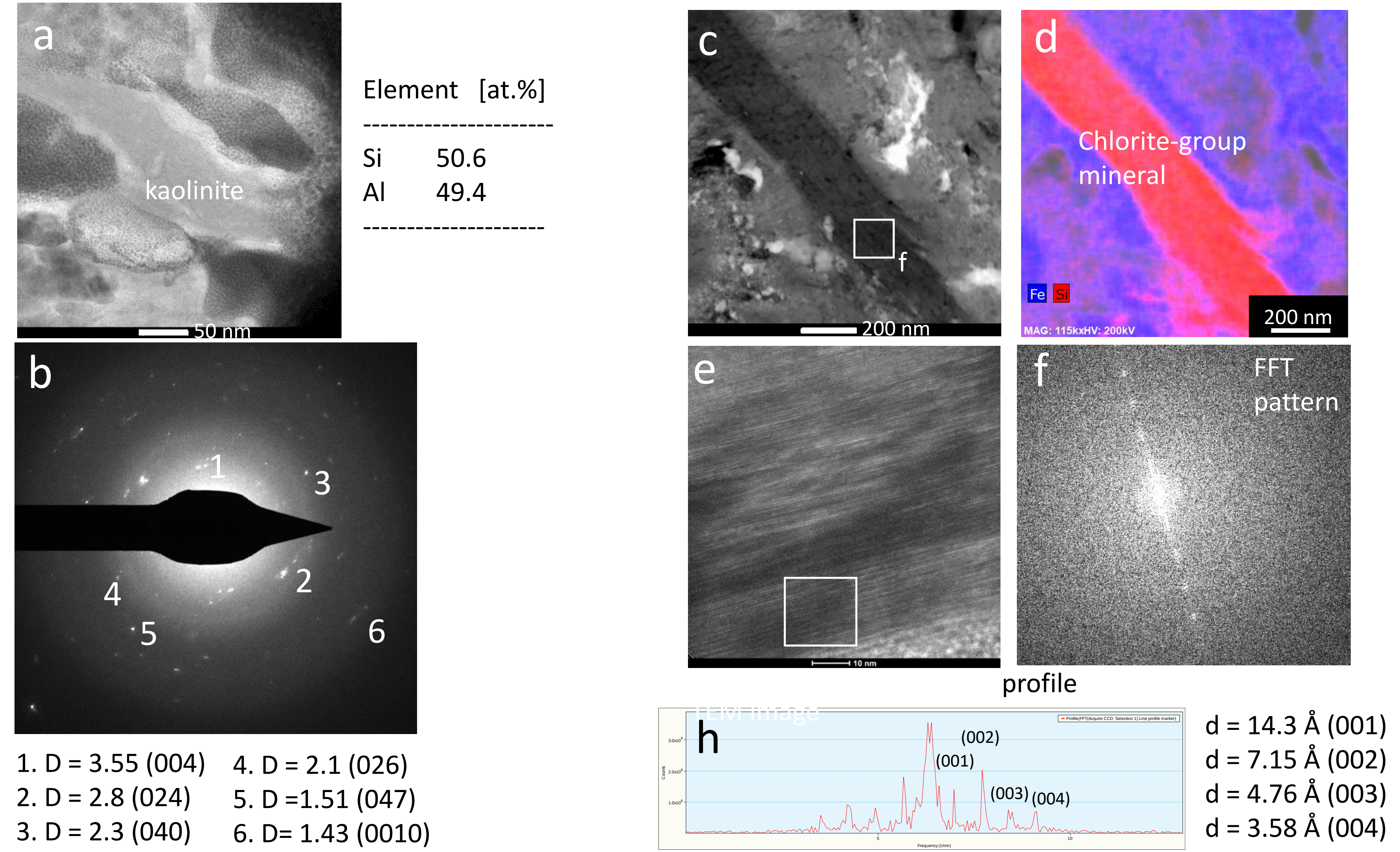

Element	[at.%]
Si	50.6
Al	49.4

1. D = 3.55 (004)
2. D = 2.8 (024)
3. D = 2.3 (040)
4. D = 2.1 (026)
5. D =1.51 (047)
6. D= 1.43 (0010)

d = 14.3 Å (001)
d = 7.15 Å (002)
d = 4.76 Å (003)
d = 3.58 Å (004)

Fig. S14 Clay minerals in lamella 1 and 2: (a) TEM image of a kaolinite lath in lamella 1 with Si:Al ratio and (b) corresponding SAED pattern with d-spacings; (c) TEM image and (d) STEM-EDS chemical distribution map for Fe (blue) and Si (red) of a chlorite lath in lamella 2; (e) HR-TEM image of the area indicated in (c); (f) FFT pattern of the area indicated in (e); (h) profile through the spots in the latter FFT pattern with corresponding d-spacings

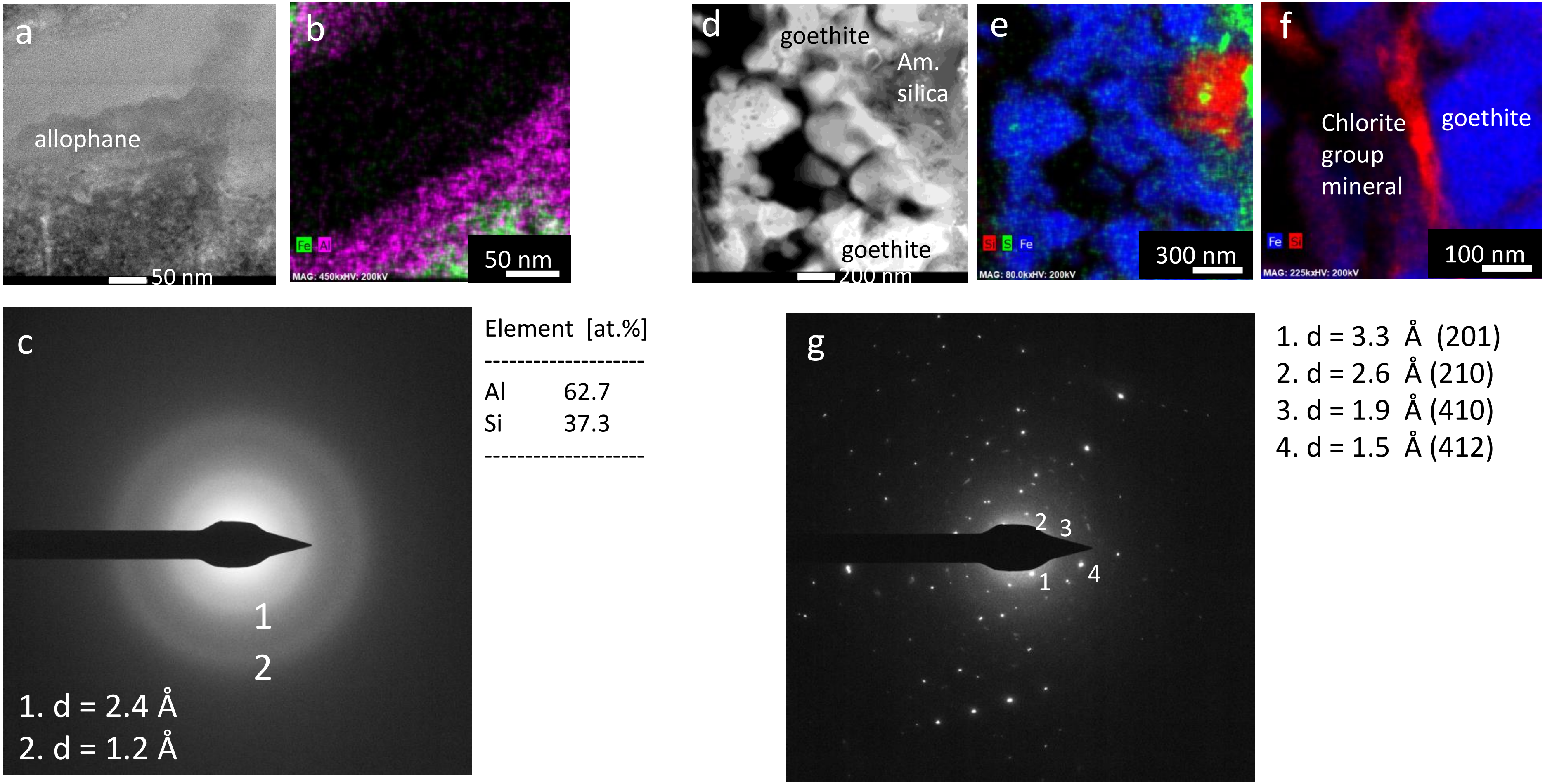

Element	[at.%]
Al	62.7
Si	37.3

1. d = 3.3 Å (201)
2. d = 2.6 Å (210)
3. d = 1.9 Å (410)
4. d = 1.5 Å (412)

Fig. S15. Allophane and bulk goethite crystals in lamella 1 and 2, respectively: (a) TEM image and (b) STEM-EDS chemical distribution map for Fe (green) and Al (violet) of a most likely allophane precipitate in the Fe-Si-rich matrix; (c) corresponding SAED pattern; Allophane and imogolite (both with Al: Si ratios of 2:1) can be commonly distinguished on the basis of their morphology with imogolite depicting a prominent tubular morphology; (d) STEM image, (e)-(f) STEM-EDS chemical distribution maps for Fe (blue) and Si (red) indicating the occurrence of bulky goethite crystals in association with amorphous silica and a chlorite-group mineral along the rim of lamella 2; (g) SAED pattern of multiple goethite crystals with d-spacings of the most prominent diffraction spots.

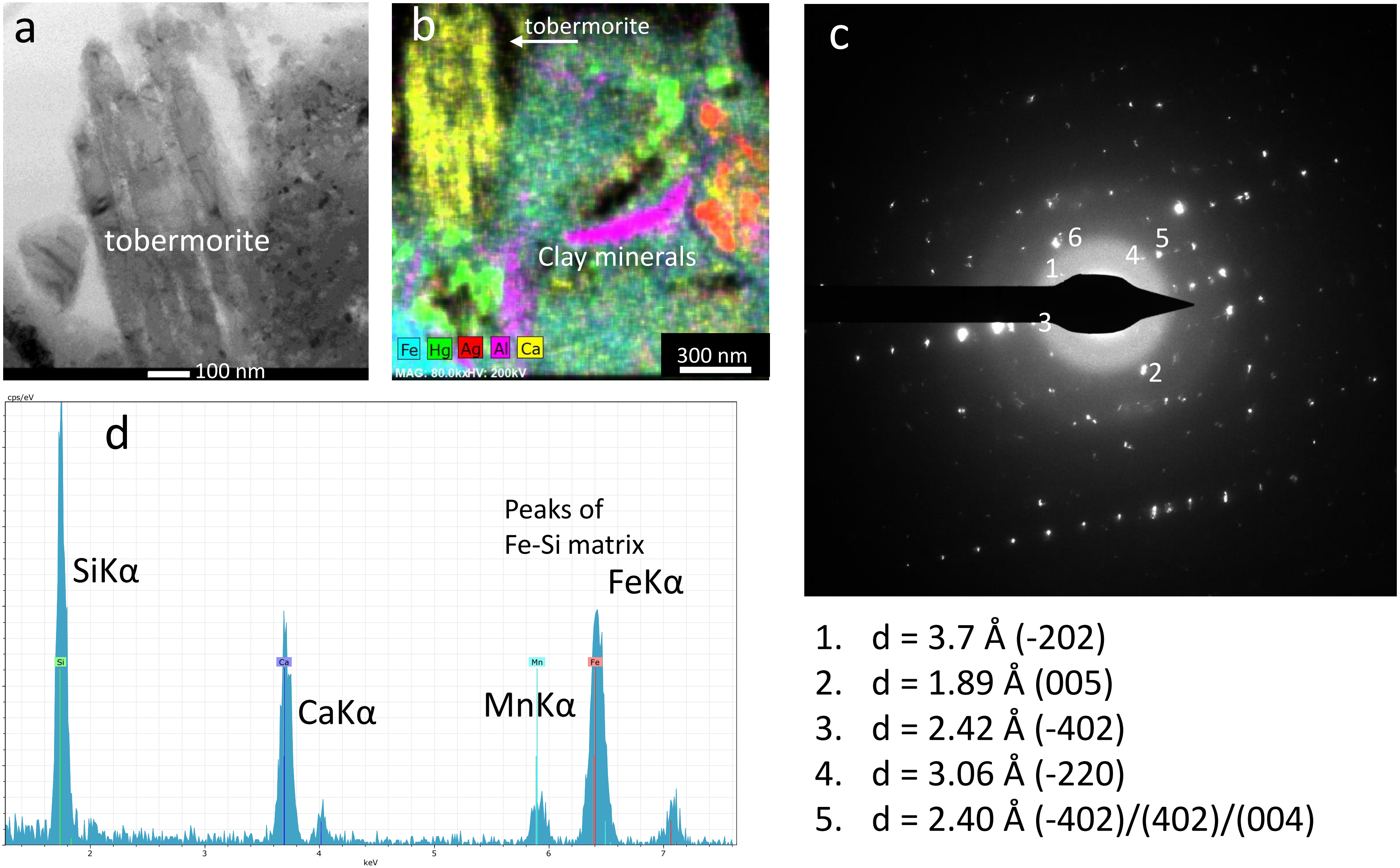

1. d = 3.7 Å (-202)
2. d = 1.89 Å (005)
3. d = 2.42 Å (-402)
4. d = 3.06 Å (-220)
5. d = 2.40 Å (-402)/(402)/(004)

Fig. S16 An assemblage of tobermorite crystals in lamella 2: (a) TEM image and (b) STEM-EDS chemical distribution map for Fe (light blue), Hg (green), Ag (red), Al (violet) and Ca (yellow); (c) SAED pattern of multiple crystals with d-spacing listed for the most prominent diffraction spots; (d) EDS spectrum; note that a chemical analysis led to a higher Si : Ca ratio (2:1) than for the ideal chemical composition of tobermorite with $Ca_4Si_6O_{15}(OH)_2 \cdot 2H_2O$, most likely due to X-ray contribution of the adjacent Fe-Si rich matrix.

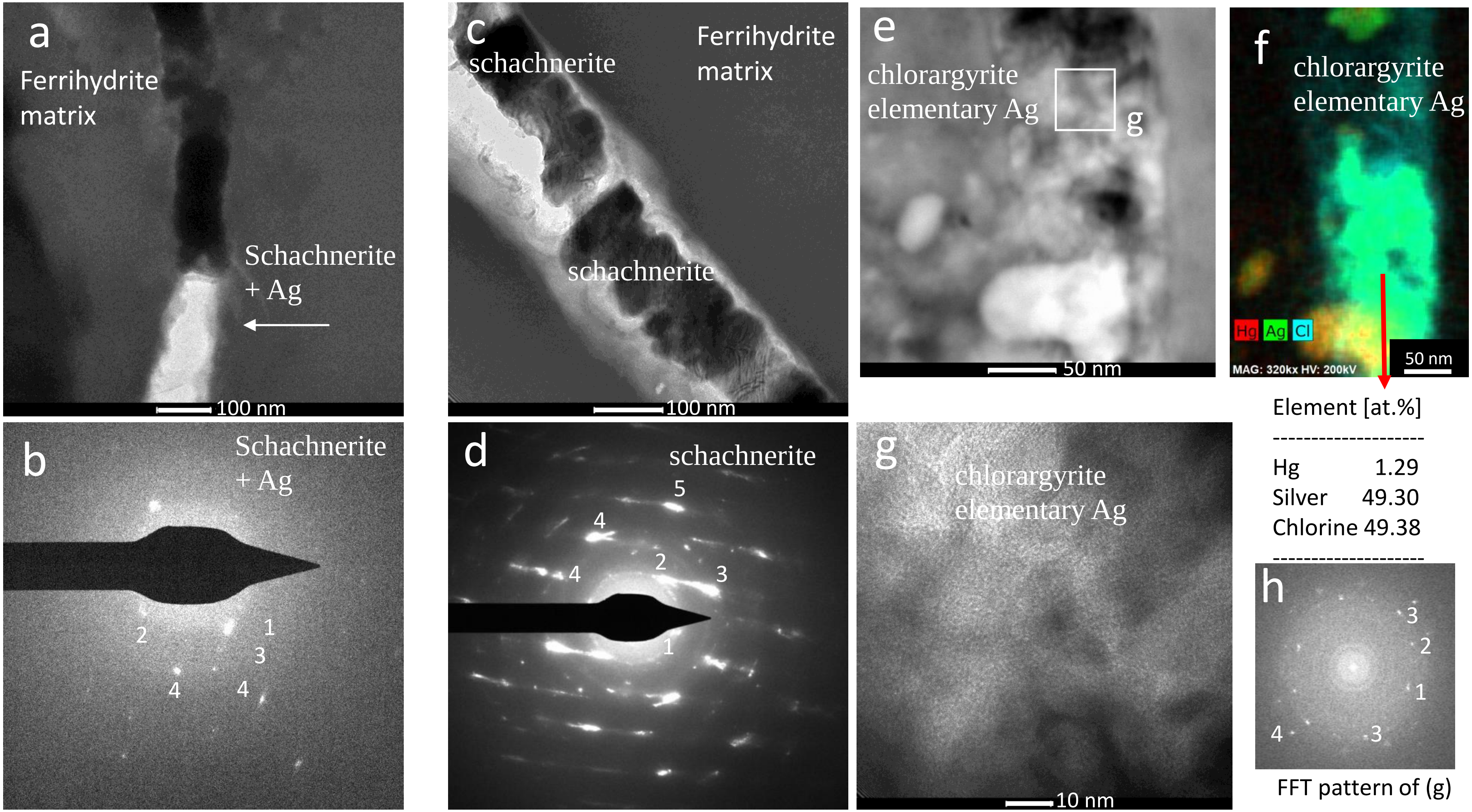

Element [at.%]

Hg 1.29

Silver 49.30

Chlorine 49.38

FFT pattern of (g)

Measured d-spacings for schachnerite (Schach) and Silver (Ag)
1. d=2.6 Å (321) schach
2. d=2.35 Å (111) Ag
3. d=2.2 Å (101)
4. d=1.5 Å (220) Ag

Measured d-spacings for schachnerite
1. d =2.6 Å(100)
2. d=2.2 Å (101)
3. d=1.35 Å (103)
4. d=1.26 Å (112)

Note: pattern of multiple crystals Ring at d =2.5 Å corresponds to ferrihydrite matrix

Measured d-spacings for chlorargyrite and elementary Ag
1. 3.0 Å (111) chlorargyrite
2. 2.7 Å (200) chlorargyrite
3. 2.35 Å (111) elementary silver
4. 1.93 Å (220) chlorargyrite